④

OFFICE OF NAVAL RESEARCH

AD-A219 436

TECHNICAL REPORT No. 6

Optical Phonons and Electronic Properties in Double Heterostructures

by

D. L. Lin, R. Chen and Thomas F. George

Prepared for Publication

in

Departments of Chemistry and Physics
State University of New York at Buffalo
Buffalo, New York 14260

March 1990

REPORT DOCUMENTATION PAGE

1a. REPORT SECURITY CLASSIFICATION Unclassified	1b. RESTRICTIVE MARKINGS
2a. SECURITY CLASSIFICATION AUTHORITY	3. DISTRIBUTION/AVAILABILITY OF REPORT Approved for public release; distribution unlimited
2b. DECLASSIFICATION/DOWNGRADING SCHEDULE	
4. PERFORMING ORGANIZATION REPORT NUMBER(S) UBUFFALO/DC/90/TR-6	5. MONITORING ORGANIZATION REPORT NUMBER(S)

6a. NAME OF PERFORMING ORGANIZATION Depts. Chemistry & Physics State University of New York	6b. OFFICE SYMBOL (If applicable)	7a. NAME OF MONITORING ORGANIZATION
6c. ADDRESS (City, State, and ZIP Code) Fronczak Hall, Amherst Campus Buffalo, New York 14260		7b. ADDRESS (City, State, and ZIP Code) Chemistry Program 800 N. Quincy Street Arlington, Virginia 22217

8a. NAME OF FUNDING/SPONSORING ORGANIZATION Office of Naval Research	8b. OFFICE SYMBOL (If applicable)	9. PROCUREMENT INSTRUMENT IDENTIFICATION NUMBER Grant N00014-90-J-1193

8c. ADDRESS (City, State, and ZIP Code) Chemistry Program 800 N. Quincy Street Arlington, Virginia 22217	10. SOURCE OF FUNDING NUMBERS			
	PROGRAM ELEMENT NO.	PROJECT NO.	TASK NO	WORK UNIT ACCESSION NO.

11. TITLE (Include Security Classification)

Optical Phonons and Electronic Properties in Double Heterostructures

12. PERSONAL AUTHOR(S)
D. L. Lin, R. Chen and Thomas F. George

13a. TYPE OF REPORT	13b. TIME COVERED FROM ____ TO ____	14. DATE OF REPORT (Year, Month, Day) March 1990	15. PAGE COUNT 15

17.	COSATI CODES		18. SUBJECT TERMS (Continue on reverse if necessary and identify by block number)
FIELD	GROUP	SUB-GROUP	OPTICAL PHONONS DOUBLE HETEROSTRUCTURES
			ELECTRONIC PROPERTIES CONINUUM MODEL
			SEMICONDUCTOR INTERFACE MODES

19. ABSTRACT (Continue on reverse if necessary and identify by block number)

Optical phonon modes in a semiconductor double heterostructure (DHS) are examined within the continuum model. The interface modes found here can account for the novel phenomena observed in right-angle Raman scattering. The Hamiltonian for the electron interaction with phonon eigenmodes is derived and employed to study polaronic effects in the DHS. The $1s$-$2p_+$ transition energy of a magnetopolaron bound a hydrogenic impurity in the quantum well is calculated, and excellent agreement with experiments is obtained.

20. DISTRIBUTION/AVAILABILITY OF ABSTRACT ☒ UNCLASSIFIED/UNLIMITED ☒ SAME AS RPT. ☐ DTIC USERS	21. ABSTRACT SECURITY CLASSIFICATION Unclassified
22a. NAME OF RESPONSIBLE INDIVIDUAL Dr. David L. Nelson	22b. TELEPHONE (Include Area Code) (202) 696-4410	22c. OFFICE SYMBOL

DD Form 1473, JUN 86   Previous editions are obsolete.   SECURITY CLASSIFICATION OF THIS PAGE

UNCLASSIFIED

Optical phonons and electronic properties in double heterostructures

D. L. Lin, R. Chen and Thomas F. George

Department of Physics and Astronomy
State University of New York at Buffalo
Buffalo, New York 14260

ABSTRACT

Optical phonon modes in a semiconductor double heterostructure (DHS) are examined within the continuum model. The interface modes found here can account for the novel phenomena observed in right-angle Raman scattering. The Hamiltonian for the electron interaction with phonon eigenmodes is derived and employed to study polaronic effects in the DHS. The $1s$-$2p_+$ transition energy of a magnetopolaron bound to a hydrogenic impurity in the quantum well is calculated, and excellent agreement with experiments is obtained.

1. INTRODUCTION

It is by now well known that in polar crystals such as III-V compounds, the electron-optical-phonon interaction plays an important role in determining the electronic properties at higher temperatures. Since these compounds are the usual materials used in the fabrication of microstructures such as heterostructures and superlattices, there has been growing interest in the study of electron-phonon interactions in these structures. Until recently, the bulk Fröhlich Hamiltonian has been employed in almost all calculations, even though the presence of surfaces and interfaces is expected to change the nature of lattice vibration modes dramatically.[1,2]
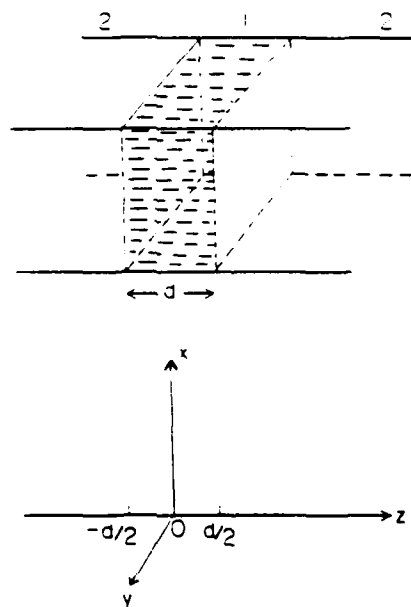
Although surface optical (SO) phonon modes have been discussed some time ago,[3,4] they have not been included until fairly recently in the treatment of polarons confined in a slab[5] or near the interface in semi-infinite systems.[6,7]

In recent papers,[8,9] the optical phonon modes in a double heterostructure (DHS) of polar crystals have been solved within the continuum model. It is found that there are only two types of phonon modes: the interface (IN) and the confined bulk modes. The latter may be either longitudinal (LO) or transversal (TO) phonon modes. Therefore, the Fröhlich Hamiltonian involving only the bulk LO phonon cannot be applied to quantum wells and other microstructures.

We report in this paper the Hamiltonian derived for the electron-optical-phonon interaction in a DHS. Both the interface and bulk LO phonons are included. The interaction Hamiltonian is then employed to study the phonon effects on electronic and optical properties in the DHS. The self-energy of a free polaron is calculated for arbitrary well width. It approaches the bulk value of the side material in the limit of $d = 0$, and that of the central layer in the limit of $d \to \infty$. For a magnetopolaron bound to a hydrogenic impurity in the GaAs/AlGaAs quantum

well, the transition energy calculated from this Hamiltonian exhibits the strange
pinning phenomena in strong magnetic fields as observed experimentally.

2. OPTICAL PHONON MODES

The detailed solution of phonon eigenmodes can be found in Refs. 8 and 9.
Here we just outline what is essential for our discussion of polaronic effects.
The geometry of our DHS is shown in Fig. 1.   Material ν ($\nu = 1,2$) is characterized

Figure 1. Geometry of the double heterostructure.

by the dielectric constants $\epsilon_\nu(\omega)$, $\epsilon_{0\nu}$ and $\epsilon_{0\infty}$, plasma frequency $\omega_{p\nu}$, number of ion
pairs n_ν per unit cell, natural frequency $\omega_{0\nu}$, and polarizability α_ν.   The
polarization vector $\vec{P}$ is related to the relative displacement $\vec{u}(\vec{r})$ of the ion pair
and to the macroscopic field $\vec{E}$

$$\vec{p}(\vec{r}) = n_\nu e^\star_\nu \eta_\nu^{-\frac{1}{2}} \vec{u}(\vec{r})$$

$$= \frac{1}{4\pi} \chi_\nu(\omega)\vec{E} \quad , \tag{1}$$

where we have defined $\eta_\nu^{\frac{1}{2}} = [1 + \alpha_\nu n_\nu (\lambda_{0\nu} - \lambda_\nu)]^{-1}$ and

$$\lambda_{0\nu} = 4\pi\omega_{0\nu}^2/\omega_{p\nu}^2 \qquad \lambda_\nu = 4\pi\omega^2/\omega_{p\nu}^2 \quad . \tag{2a,b}$$

The dielectric susceptibility $\chi_\nu(\omega)$ is given by

$$4\pi\chi_\nu^{-1} = (\lambda_{0\nu} - \lambda_\nu)\eta_\nu^{\frac{1}{2}} - 4\pi/3 \tag{3}$$

and is related to the dielectric function by $\chi_\nu(\omega) = \epsilon_\nu(\omega) - 1$. With the frequency parameters (2), we find from (3)

$$\epsilon_\nu(\omega) = \epsilon_{\infty\nu}(\omega_{L\nu}^2 - \omega^2)/(\omega_{T\nu}^2 - \omega^2) \tag{4a}$$

$$\epsilon_{\infty\nu} = 1 + 4\pi n_\nu \alpha_\nu/(1 - \frac{4\pi}{3} n_\nu \alpha_\nu) \quad . \tag{4b}$$

The electrostatic potential $\phi(\vec{r})$ that gives rise to the field $\vec{E}$ satisfies

$$\vec{E}(\vec{r}) = -\nabla\phi(\vec{r}) \quad . \tag{5}$$

On the assumption that the dielectric function $\epsilon_\nu(\omega)$ does not depend upon the spatial coordinates within each layer, we have from (5) and $\nabla\cdot\vec{D} = 0$

$$\epsilon_\nu(\omega)\nabla^2\phi(\vec{r}) = 0 \quad . \tag{6}$$

Since the DHS does not possess translational invariance in the z-direction, the two-dimensional (2D) vectors $\vec{\kappa}$ and $\vec{\rho}$ are introduced in the wave vector $\vec{k} = (\vec{\kappa},q)$ and in the position vector $\vec{r} = (\vec{\rho},z)$. The potential can then be written as

$$\phi(\vec{r}) = \int d\vec{\kappa} \, \phi(\vec{\kappa},z)e^{i\vec{\kappa}\cdot\vec{\rho}} \quad . \tag{7}$$

Substituting (7) in (6), we find that the Fourier components of the potential satisfy the equation

$$\epsilon_\nu(\omega) \left[\frac{\partial^2}{\partial z^2} - \kappa^2\right] \phi(\vec{\kappa},z) = 0 \quad , \tag{8}$$

which may be solved by assuming either

$$\epsilon_\nu(\omega) = 0 \quad , \quad \nu = 1,2 \tag{9a}$$

or

$$\left[\frac{\partial^2}{\partial z^2} - \kappa^2\right] \phi(\vec{\kappa},z) = 0 \quad . \tag{9b}$$

It is seen from (4a) that (9a) is satisfied by the LO frequencies $\omega^2 = \omega_{L\nu}^2$. Because $\omega_{L1} \neq \omega_{L2}$, the vibrations on both sides of the interface have different time dependences. The boundary conditions that both ϕ and the electric displacement D_z must be continuous across the interfaces then require the confinement of the LO modes. On the other hand, Eq. (9b) yields the interface modes of vibration. The polarization eigenvectors of all these modes as well as the dispersion relations have been worked out in Ref. 8. It is also shown there that the novel slab modes observed in right-angle Raman scattering[10] can be interpreted as the interface modes. As discussed in Ref. 8, in the vicinity of the center of the first Brillouin zone, the antisymmetric interface modes, which are predominantly transversal, oscillate at longitudinal frequency while the symmetric interface modes are longitudinal but oscillate at transversal frequency. Using Eqs. (8) and (9), we find after a straightforward calculation electrostatic potentials corresponding to these modes. Thus for the confined LO modes, the Fourier components of the potential are

$$\phi_m(\vec{\kappa},z) = 4\pi C_m(\vec{\kappa}) \begin{cases} \sin(m\pi z/d) & , \quad \text{for even } m \\ \cos(m\pi z/d) & , \quad \text{for odd } m \end{cases} \tag{10a}$$

with the normalization constant

$$|C_m(\kappa)| = \omega_{p\nu} \eta_\nu^{-\frac{1}{2}} \sqrt{2/d} \, [\kappa^2 + (m\pi/d)^2]^{2-\frac{1}{2}} \,. \tag{10b}$$

Corresponding to the interface modes, the potentials are

$$\phi_{sj}(\vec{\kappa}\cdot z) = \begin{cases} C_{sj} e^{-\kappa|z|} & , \quad |z| > d/2 \\ C_{sj}(1 + \epsilon_2/\epsilon_1) \cosh(\kappa z) & , \quad |z| < d/2 \end{cases} \tag{11a}$$

for the symmetric modes and

$$\phi_{aj}(\vec{\kappa}\cdot z) = \begin{cases} -C_{aj} \text{sgn}(z) \, e^{-\kappa|z|} & , \quad |z| > d/2 \\ C_{aj}(1 + \epsilon_2/\epsilon_1) \sinh(\kappa z) & , \quad |z| < d/2 \end{cases} \tag{11b}$$

for the antisymmetric modes. The function $\text{sgn}(z) = 1$ for $z > 0$ and -1 for $z < 0$. The index $j = 1,2$ in Eq. (11) labels the two branches of the symmetric or antisymmetric interface modes which have the same normalization constant as discussed in Ref. 8. The normalization constants are given by

$$|C_{sj}(\vec{\kappa})| = \frac{4\pi}{\sqrt{A}} \, \epsilon^{\kappa d/2} \Big/ \left\{ 2\kappa \left[\frac{\eta_1 \chi_1^2}{\omega_{p1}^2} \tan(\frac{\kappa d}{2}) + \frac{\eta_2 \chi_2^2}{\omega_{p2}^2} \right] \right\}^{\frac{1}{2}} \tag{12a}$$

$$|C_{aj}(\vec{\kappa})| = \frac{4\pi}{\sqrt{A}} e^{\kappa d/2} \overline{\sqrt{\tanh(\frac{\kappa d}{2})}} \Big/ \left\{ 2\kappa \left[\frac{\eta_1 \chi_1^2}{\omega_{p1}^2} + \frac{\eta_2 \chi_2^2}{\omega_{p2}^2} \tanh(\frac{\kappa d}{2}) \right] \right\}^{\frac{1}{2}} \quad . \qquad (12b)$$

3. ELECTRON-PHONON INTERACTIONS

To derive the Hamiltonian operator, we start with the free polarization or the free phonon. In terms of the polarization vector $\vec{\pi}$ and its canonical conjugate $\dot{\vec{\pi}}$, we can write the Hamiltonian in the form

$$H_{ph} = \frac{1}{2} \sum_\alpha \int d\vec{r} \, \frac{4\pi\eta_\nu}{\omega_{p\nu}^2} \, [\dot{\pi}_\alpha^*(\vec{r})\dot{\pi}_\alpha(\vec{r}) + \omega^2 \pi_\alpha^*(\vec{r})\pi_\alpha(\vec{r})] \quad . \qquad (13)$$

$\vec{\pi}$ and $\dot{\vec{\pi}}$ can be regarded as quantum mechanical operators and can be expressed in terms of their Fourier components as

$$\vec{\pi}(\vec{r}) = \sum_{\vec{\kappa},m} \overline{\sqrt{\hbar/8\pi A\omega_{L\nu}}} \, [a_m(\vec{\kappa}) + a_m^\dagger(-\vec{\kappa})]\vec{\pi}_m(\vec{r})$$

$$+ \sum_{\vec{\kappa},j} \left\{ \overline{\sqrt{\hbar/8\pi A\omega_{sj}(\vec{\kappa})}} \, [a_{sj}(\vec{\kappa}) + a_{sj}^\dagger(-\kappa)]\vec{\pi}_{sj}(\vec{r}) \right.$$

$$+ \left. \overline{\sqrt{\hbar/8\pi A\omega_{aj}(\vec{\kappa})}} \, [a_{aj}(\vec{\kappa}) + a_{aj}^\dagger(-\vec{\kappa})]\vec{\pi}_{aj}(\vec{r}) \right\} \qquad (14a)$$

$$\dot{\vec{\pi}}(\vec{r}) = \sum_{\vec{\kappa},m} i\overline{\sqrt{\hbar\omega_{L\nu}/8\pi A}} \, [a_m(\vec{\kappa}) - a_m^\dagger(\vec{\kappa})]\vec{\pi}_m(\vec{r})$$

$$+ \sum_{\vec{\kappa},j} \left\{ i\overline{\sqrt{\hbar\omega_{sj}(\vec{\kappa})/8\pi A}} \, [a_{sj}(\vec{\kappa}) - a_{sj}^\dagger(-\vec{\kappa})]\vec{\pi}_{sj}(\vec{r}) \right.$$

$$+ \left. i\overline{\sqrt{\hbar\omega_{aj}(\vec{\kappa})/8\pi A}} \, [a_{aj}(\vec{\kappa}) - a_{aj}^\dagger(-\vec{\kappa})] \, \vec{\pi}_{aj}(\vec{r}) \right\} \quad . \qquad (14b)$$

In Equations (14), we have introduced the area A of the interface, and the creation (annihilation) operators $a_m^\dagger(\vec{\kappa})$ $(a_m(\vec{\kappa}))$ for the confined modes and $a_{sj,aj}^\dagger(\vec{\kappa})$ $(a_{sj,aj}(\vec{\kappa}))$ for the symmetric and antisymmetric interface modes of phonons. They obey the commutation relations

$$[a_\alpha(\vec{\kappa}), a_\beta^\dagger(\vec{\kappa}')] = \delta_{\alpha\beta}\ \delta(\vec{\kappa}-\vec{\kappa}') \tag{15a}$$

$$[a_\alpha^\dagger(\vec{\kappa}),\ a_\beta^\dagger(\vec{\kappa}')] = [a_\alpha(\vec{\kappa}), a_\beta(\vec{\kappa}')] = 0\ \ . \tag{15b}$$

Using these commutators as well as the orthonormality relation for the eigenvectors, it is straightforward to show that

$$H_{ph} = H_{LO} + H_{IN} \tag{16a}$$

$$H_{LO} = \sum_{\vec{\kappa},m} \hbar\omega_{L\nu}\ [a_m^\dagger(\vec{\kappa})a_m(\vec{\kappa}) + \tfrac{1}{2}] \tag{16b}$$

$$H_{IN} = \sum_{\vec{\kappa},j} \left\{ \hbar\omega_{sj}(\vec{\kappa})[a_{sj}^\dagger(\vec{\kappa})\ a_{sj}(\vec{\kappa}) + \tfrac{1}{2}] + \hbar\omega_{aj}(\vec{\kappa})[a_{aj}^\dagger(\vec{\kappa})a_{aj}(\vec{\kappa}) + \tfrac{1}{2}] \right\}\ \ . \tag{16c}$$

The interaction energy for an electron interacting with the polarization at a point $\vec{r}$ is represented by the Hamiltonian

$$H_{e\text{-}ph} = -\ e\phi(\vec{r})\ \ . \tag{17}$$

Regarded as a quantum mechanical operator, the scalar field can be expressed, with the help of (1), (4) and (5), as

$$\phi(\vec{r}) = \sum_{\vec{\kappa},m} \overline{\sqrt{\hbar/8\pi A\omega_{L\nu}}}\ [a_m(\vec{\kappa}) + a_m^\dagger(-\vec{\kappa})]\phi_m(\vec{r})$$

$$+ \sum_{\vec{\kappa},j} \left\{ \overline{\sqrt{\hbar/8\pi A\omega_{sj}(\vec{\kappa})}}\ [a_{sj}(\vec{\kappa}) + a_{sj}^\dagger(-\vec{\kappa})]\phi_{sj}(\vec{r}) \right.$$

$$\left. + \overline{\sqrt{\hbar/8\pi A\omega_{aj}(\vec{\kappa})}}\ [a_{aj}(\vec{\kappa}) + a_{aj}^\dagger(-\vec{\kappa})]\phi_{aj}(\vec{r}) \right\}\ \ . \tag{18}$$

Combining (10a), (11) and (18), we find after some algebra the interaction Hamiltonian

$$H_{e\text{-}ph} = H_{e\text{-}LO} + H_{e\text{-}IN} \tag{19}$$

$$H_{e\text{-}LO} = -\ \sum_{\vec{\kappa}} e^{i\vec{\kappa}\cdot\vec{\rho}} \left\{ \sum_{m=1,3\ldots} B_m(\kappa)\ \cos(\tfrac{m\pi z}{d})[\hat{a}_m(\vec{\kappa}) + \hat{a}_m^\dagger(-\vec{\kappa})] \right.$$

$$+ \sum_{m=2,4\ldots} B_m(\kappa)\ \sin(\frac{m\pi z}{d})\,[\hat{a}_m(\vec{\kappa}) + \hat{a}_m^\dagger(-\vec{\kappa})]\Bigg\} \qquad (20)$$

$$H_{e-IN} = -\sum_{\vec{\kappa},j} e^{i\vec{\kappa}\cdot\vec{\rho}-\kappa(|z|-d/2)} \Bigg\{ B_{sj}(\vec{\kappa})\,[\hat{a}_{s,j}(\vec{\kappa}) + \hat{a}_{s,j}^\dagger(-\vec{\kappa})]$$

$$- sgn(z)B_{aj}(\kappa)[\hat{a}_{a,j}(\vec{\kappa}) + \hat{a}_{a,j}^\dagger(-\vec{\kappa})]\Bigg\} \qquad \text{for } |z| > d/2 \qquad (21a)$$

$$H_{e-IN} = -\sum_{\vec{\kappa},j} e^{i\vec{\kappa}\cdot\vec{\rho}}\Bigg\{ B_{sj}(\kappa)\,\frac{\cosh(\kappa z)}{\cosh(\kappa d/2)}\,[\hat{a}_{s,j}(\vec{\kappa}) + \hat{a}_{s,j}^\dagger(-\vec{\kappa})]$$

$$- B_{aj}(\kappa)\,\frac{\sinh(\kappa z)}{\sinh(\kappa d/2)}\,[\hat{a}_{a,j}(\vec{\kappa}) + \hat{a}_{a,j}^\dagger(-\vec{\kappa})]\Bigg\} \qquad \text{for } |z| < d/2 \;.$$
$$(21b)$$

The coefficients can be calculated from (10b) and (12). The results are

$$|B_m(\vec{\kappa})|^2 = \frac{e^2\hbar}{8\pi A\omega_{L\nu}}\ |C_m(\vec{\kappa})|^2 = \frac{4\pi e^2\hbar\omega_{L\nu}}{Ad(\kappa^2 + \frac{m\pi}{d})}\left[\frac{1}{\epsilon_{\infty\nu}} - \frac{1}{\epsilon_{o\nu}}\right] \qquad (22a)$$

$$|B_{sj,aj}(\vec{\kappa})|^2 = \frac{e^2\hbar}{8\pi A\omega_{sj,aj}(\vec{\kappa})}\ e^{-\kappa d}\ |C_{sj,aj}(\vec{\kappa})|^2 \;, \qquad (22b)$$

which leads to

$$|B_{sj}(\vec{\kappa})|^2 = \frac{\pi e^2}{A\kappa} - \hbar\omega_{sj}(\vec{\kappa})/[\bar{\epsilon}_1\tanh(\frac{\kappa d}{2}) + \bar{\epsilon}_2] \qquad (23a)$$

$$|B_{aj}(\vec{\kappa})|^2 = \frac{\pi e^2}{A\kappa} - \hbar\omega_{aj}(\vec{\kappa})/[\bar{\epsilon}_1\coth(\frac{\kappa d}{2}) + \bar{\epsilon}_2] \;. \qquad (23b)$$

For convenience, we have defined in (23) the dielectric functions $\bar{\epsilon}_\nu(\omega)$ by

$$\frac{1}{\bar{\epsilon}_\nu(\omega)} = \frac{1}{\epsilon_\nu(\omega) - \epsilon_{o\nu}} - \frac{1}{\epsilon_\nu(\omega) - \epsilon_{\infty\nu}} \;. \qquad (24)$$

4. POLARON IN A DHS

We now proceed to calculate the polaron self-energy by perturbation theory. The unperturbed ground-state wave function is taken to be

$$|\psi_o> = |\vec{k},0; n_{\vec{\kappa},\beta}> = \frac{1}{\sqrt{A}}\, e^{i\vec{k}\cdot\vec{\rho}}\, f(z)\, |n_{\vec{\kappa},\beta}> \quad , \tag{25}$$

where electron states are characterized by a plane wave $\vec{k}$ in the xy-plane and the ground state 0 in the z-direction. The electron wave vector is defined as $\vec{k}_e = (\vec{k},k_z)$ and the electron ground state wave function in a quantum well is given by

$$f(z) = \begin{cases} C\,\cos(k_z d/2)\,\exp[ik_z'(|z|-d/2)] & , \quad |z| \geq d/2 \\ C\,\cos(k_z z) & , \quad |z| < d/2 \end{cases} \quad . \tag{26}$$

The wave numbers k_z and k_z' are related to the electron subband energy E_ℓ by

$$k_z = \sqrt{2m_e E_\ell/\hbar^2} \quad , \quad k_z' = \sqrt{2m_e(V_o-E_\ell)/\hbar^2} \tag{27}$$

with E_ℓ determined by the transcendental equation

$$E_\ell = V_o\,\cos^2(\frac{d}{2}\sqrt{2m_e E_\ell/\hbar^2}) \quad , \quad \ell = 1,\, 2,\, \ldots \tag{28}$$

The normalization constant C is given by

$$C = \sqrt{2k_z'/(k_z'd + 2)} \quad . \tag{29}$$

The phonon state $|n_{\vec{k},\beta}>$ is specified by n phonons with wave vector $\vec{k} = (\vec{\kappa},q)$ and index β labeling the phonon mode, which may be one of the interface or confined LO modes.

The unperturbed energy of the electron in the ground state (25) can be written as

$$\epsilon_{\vec{k}_e}^{(0)} = \frac{\hbar k^2}{2m_e} + E_\ell + \sum_{\vec{\kappa},\beta}(n+\frac{1}{2})\,\hbar\omega_{\vec{\kappa},\beta} \quad . \tag{30}$$

In the weak-coupling approximation, the corrections due to the electron-phonon interaction can be calculated by standard perturbation theory as

$$\epsilon_{\vec{k}_e} - \epsilon_{\vec{k}_e}^{(0)} = \sum_{\vec{\kappa},\beta} |<\vec{k},1_{\vec{\kappa},\beta}|H_{e-ph}|\vec{k}-\vec{\kappa},0_{\vec{\kappa},\beta}>|^2 / \left[\epsilon_{\vec{k}}^{(0)} - \epsilon_{\vec{k}-\vec{\kappa}}^{(0)} - \hbar\omega_{\vec{\kappa},\beta}\right]$$

$$= \Delta E_1 + \Delta E_2 + \Delta E_3 \quad , \tag{31}$$

where we have assumed that transistions to or from a state with more than one phonon are negligible. Because we are only interested in the electron self-energy due to electron-phonon interactions, matrix elements corresponding to interband transitions are all ignored. With the Hamiltonian operators given by (19)-(21), and the wave function by (25), we find, after integration over the phonon momentum, that

$$\Delta E_1 = -\alpha_{L1}\hbar\omega_{L1} - \gamma_{L1}\,\hbar^2 k^2/2m_e \tag{32a}$$

$$\Delta E_2 = -\alpha_{L2}\hbar\omega_{L2} - \gamma_{L2}\,\hbar^2 k^2/2m_e \tag{32b}$$

$$\Delta E_3 = -\sum_j \int_0^\infty d\kappa\,\alpha_{IN}(\kappa)\hbar\omega_{sj}(\kappa) - \gamma_{IN}\,\hbar^2 k^2/2m_e \quad . \tag{32c}$$

The parameters α and γ are related to the Fröhlich-type coupling constants involving the particular phonon modes indicated by the subscripts. Explicitly, the α's are given by

$$\alpha_{L1} = \frac{4\alpha_{F1}}{K_{p1}d}\,|C|^4 \sum_{m=1,3\ldots} \left(\frac{d}{m\pi}\right)^2\left[1 + \frac{\cos(k_z d)}{1 - \left(\frac{2k_z d}{\mu\pi}\right)^2}\right]\left[\left(\frac{\pi}{K_{p1}d}\right)^2 - 1\right]^{-1}\ell n\left|\frac{m\pi}{K_{p1}d}\right| \tag{33a}$$

$$\alpha_{L2} = \frac{4\alpha_{F2}}{\pi K_{p2}^2}\,|C|^4\cos^4(k_z d/2)\int_0^\infty dt\,\frac{t^2\ell n|t|}{[t^2 + 4(k_z'/K_{p2})^2]^2(t^2-1)} \tag{33b}$$

$$\alpha_{IN} = \alpha_{Fsj}(\kappa)\,|C|^4/K_{psj}(\kappa)Q^2(\kappa)\left[\left(\frac{\kappa}{K_{psj}(\kappa)}\right)^2 + 1\right] \quad , \tag{33c}$$

and we have defined the function

$$Q^{-1}(\kappa) = \frac{2\cos^2(k_z d/2)}{\kappa + 2k_z'} + \frac{\tanh(\kappa d/2)}{\kappa} + \frac{2k_z\sin(k_z d)}{\kappa^2 + 4k_z^2}$$

$$+ \frac{\kappa}{\kappa^2 + 4k_z^2}\tanh\left(\frac{\kappa d}{2}\right)\cos(k_z d) \quad . \tag{34}$$

K_{p1}^{-1} and K_{p2}^{-1} measure the polaron size due to the LO phonon in materials 1 and 2, respectively, while α_{F1} (α_{F2}) denotes the usual LO-phonon-electron coupling constant of the Frölich type in material 1 (2). They are given by

$$\gamma_{L1} = \frac{4\alpha_{F1}}{K_{p1}d} |C|^4 \sum_{m=1,3,\ldots} \left(\frac{d}{m\pi}\right)^2 \left[1 + \cos(k_z d)/\{1 - \frac{2k_z d}{m\pi}\}\right]^2$$

$$\times \int_0^\infty dt\ t/\left[t + \left(\frac{m\pi}{K_{p1}d}\right)^2\right](t+1)^3 \tag{35a}$$

$$\gamma_{L2} = \frac{\alpha_{F2}}{k_z' K_{p2}} \cos^4(k_z d/2) \int_0^\infty dt\ t/(\sqrt{t} + 2k_z'/K_{p2})^2(t+1)^3 \tag{35b}$$

$$\gamma_{IN} = \sum_j \int_0^\infty d\kappa\ 2\kappa^2 \alpha_{Fsj}(\kappa)|C|^4/K_{psj}^3 Q^2(\kappa)[(\kappa/K_{psj})^2 + 1]^3 \quad . \tag{35c}$$

Substituting Eqs. (32) into (31) we find

$$\epsilon_{\vec{k}_e} - \epsilon_{\vec{k}_e}^{(0)} = -\alpha_{L1}\hbar\omega_{L1} - \alpha_{L2}\hbar\omega_{L2} - \sum_j \int_0^\infty d\kappa\ \alpha_{IN}(\kappa)\hbar\omega_{sj}(\kappa)$$

$$- \frac{\hbar^2 k^2}{2m_e} (\gamma_{L1} + \gamma_{L2} + \gamma_{IN}) \quad . \tag{36}$$

Combining (36) and the unperturbed energy (30), we obtain immediately the ground-state energy of the interacting electron-phonon system as

$$\epsilon_{\vec{k}_e} = \frac{\hbar^2 k^2}{2m_e^\star} + E_\ell + \sum_{\vec{\kappa},\beta} (n + \frac{1}{2})\ \hbar\omega_{\kappa,\beta} - \Delta E \quad , \tag{37}$$

where

$$m_e^\star = m_e/(1 - \gamma_{L1} - \gamma_{L2} - \gamma_{IN}) \tag{38}$$

is the polaron effective mass and

$$\Delta E = \alpha_{L1}\hbar\omega_{L1} + \alpha_{L2}\hbar\omega_{L2} + \sum_j \int_0^\infty d\kappa\ \alpha_{IN}(\kappa)\hbar\omega_{sj}(\kappa) \tag{39}$$

Equation (39) is now employed to compute the binding energy of a polaron in the GaAs quantum well of a GaAs/AℓAs double heterostructure. The results are plotted as a function of the well width d in Fig. 2 in which contributions from the confined LO modes and interface modes are shown by dotted and dashed lines, respectively.
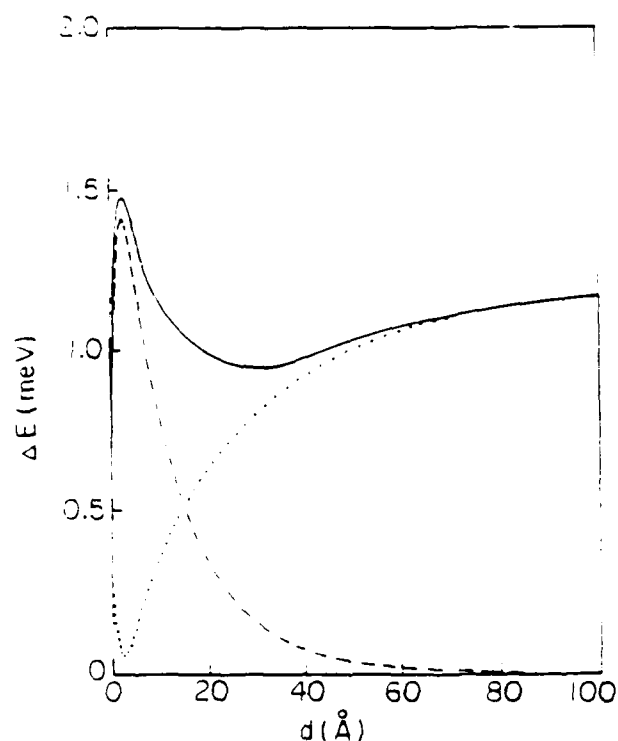
Figure 2. Polaron binding energy as a function of the
well width. The dotted and dashed lines represent the
contributions from confined LO and interface modes,
respectively.

It is observed that for small d, our results are qualitatively different from
what can be found in the literature. In fact, this is the first calculation that
gives in the limit of d – 0 the correct self-energy , the corresponding value in
material 2. This is because we have included the contribution from confined LO
phonons in material 2 in our Hamiltonian. The interface modes play an important
role in the small-d regime. Their influence quickly diminishes as d increases. It
is important to note that interface phonons are responsible for the pinning effect
observed in a quantum well on the transition energy of the polaron bound to a
hydrogenic impurity.[11] This is discussed in the following section.

5. TRANSITION ENERGY OF A BOUND MAGNETOPOLARON

Recent experiments[11,12] reveal that the resonant effect of the electron-
phonon-interaction on the 1s-2p transition energy of a magnetopolaron bound to a
hydrogenic impurity in GaAs/AlGaAs multiple-quantum-well structures exhibits the
pinning phenomenon at an energy below the TO-phonon energy. To our knowledge, the
origin of this surprising effect has not been understood.[13] Here we attempt to
calculate this transition energy in the GaAs well of a GaAs/AlGaAs DHS.

Consider a donor impurity at the center of the well as in the case of the
sample used in the experiments. A magnetic field is applied along the axis of the
quantum well. The total Hamiltonian can be written as

$$H = H_e + H_{ph} + H_{e\text{-}ph} \quad , \tag{40}$$

where

$$H_e = [\vec{p} - \frac{e}{c}\vec{A}]/2m_e - \frac{e^2}{\epsilon_o r} + V_B(z) \tag{41a}$$

represents the energy of a hydrogenic impurity confined in the square well given by

$$V_B(z) = \begin{cases} 0 & , & |z| \leq d/2 \\ V_o & , & |z| > d/2 \end{cases} \quad , \tag{41b}$$

the free phonon energy H_{ph} is given by (16) and the interaction $H_{e\text{-}ph}$ by (19)-(21).

The unperturbed energy levels of the hydrogenic impurity described by (41a) are calculated variationally. For the trial wave function, we take

$$\psi = f(z) \, G(\rho, z, \phi) \quad . \tag{42}$$

The function $f(z)$ is the solution to the square-well problem and is given by

$$f(z) = \begin{cases} \cos(k_z z) & , & z \leq d/2 \\ \\ Ae^{-k_z' z} & , & z > d/2 \end{cases} \quad , \tag{43}$$

where k_z and k_z' are defined in (27) with E_ℓ representing the energy of the first subband. The function $G(\rho, z, \phi)$ describes the internal states of the donor and is chosen to reflect the symmetry properties of the system,

$$G(\rho, z, \phi) = \rho^{|m|} \, e^{im\phi} \, e^{-\gamma\rho^2/4} \, e^{-\gamma\xi^2 z^2/4} \quad , \tag{44}$$

where ξ is the variational parameter to be determined by minimizing the ground-state energy.

The interaction $H_{e\text{-}ph}$ is then treated as a perturbation, and the energy levels are calculated by means of Wigner-Brillouin perturbation theory. The result is[14]

$$E_i(B) = E_i(B) + \frac{1}{(2\pi)^2} \sum_n \int d^2\kappa \, \frac{|\langle n|H_{e\text{-}ph}|i\rangle|^2}{E_i(B) - E_n(B) - \hbar\omega(\vec{\kappa})} \quad , \tag{45}$$

where $E_i(B)$ stands for the corresponding unperturbed energy. The calculation is rather complicated, and detailed discussion of the procedures will be published elsewhere.[15] Here we just mention that the Hilbert space has been truncated to only the lowest three states in our second-order perturbation term. In other words, only 1s, $2p_+$ and $2p_-$ are included. For the particular samples used in these

experiments,[11,12] all other states including $2p_o$ are pushed up by the quantum well way too high because of the broken symmetry and cannot be reached with presently-available magnetic fields. Furthermore, interactions of the electron with lattice vibrations outside the well under consideration are ignored, since they are important only for a very narrow (d $\leq$ 10 Å) well, while d is larger than 100 Å in the experiments considered here.
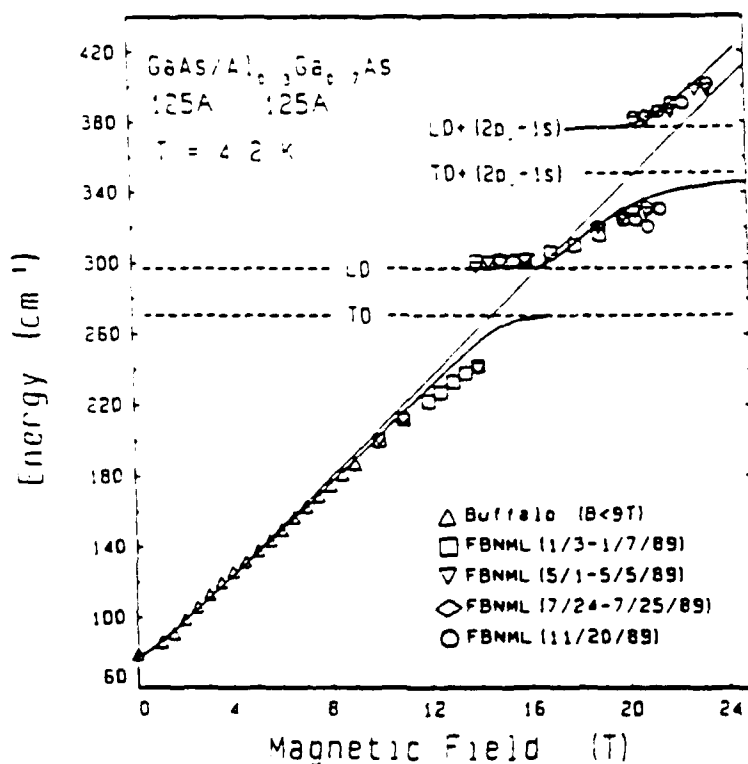

Figure 3. 1s-2p$_+$ transition energy as a function of the magnetic field B. Data are taken at SUNY-Buffalo and at the Francis Bitter National Magnet Laboratory in a series of measurements as indicated at the lower right corner. The heavy solid line represent results from the present theory and the straight line is the result without electron-phonon interaction.

The 1s-2p$_+$ transition energy calculated by computer iteration is plotted as a function of the field B in Fig. 3 along with the newly-improved set of data.[12] It is remarkable that the theoretical curve breaks into three branches separated by two gaps, in good agreement with experiments. The occurrence of gaps reflects the energy level repelling caused by the strong resonance interaction when the transition energy matches the phonon energy. Since the electron does not couple to TO-phonons, this pinning phenomenon must be due to the electron interaction with interface phonons which oscillate at frequencies between the bulk ω_L and ω_T. The

interface-phonon coupling alone, however, is not adequate for a complete understanding of this phenomenon. There are still small discrepancies between experimental data and the theory, especially in the lower branch near the gap. Minor corrections such as the nonparabolic effect on the effective mass can probably account for the discrepancies. This and other possible corrections will be discussed in a forthcoming article.[15]

6. ACKNOWLEDGMENTS

7. REFERENCES

1. R. Lassnig, Phys. Rev. B 30, 7132 (1984).
2. L. Wendler, Phys. Stat. Solidi B 129, 513 (1985).
3. R. Fuchs and K. L. Kliewer, Phys. Rev. 140, A2076 (1965).
4. J. J. Licari and Evrard, Phys. Rev. B 15, 2254 (1977).
5. X. X. Liang, S. W. Gu and D. L. Lin, Phys. Rev. B 34, 1251 (1986).
6. C. Y. Chen, T. Z. Ding and D. L. Lin, Phys. Rev. B 35, 4398 (1987); C. Y. Chen, D. L. Lin and T. Z. Ding, Phys. Rev. B 36, 9816 (1987).
7. S. W. Gu, X. J. Kong and C. W. Wei, Phys. Rev. B 36, 7977 (1987).
8. R. Chen, D. L. Lin and T. F. George, Phys. Rev. B 41, 1435 (1990); D. L. Lin, R. Chen and T. F. George, Solid State Commun. (in press).
9. N. Mori and T. Ando, Phys. Rev. 40, 6175 (1989).
10. J. E. Zucker, A. Pinczuk, D. S. Chemla, A. Gossard and W. Wiegmann, Phys. Rev. Lett. 53, 1280 (1984).
11. Y. H. Change, B. D. McCombe, J. M. Mercy, A. A. Reeder, J. Ralston and G. A. Wicks, Phys. Rev. Lett. 61, 1408 (1988).
12. J. P. Cheng, B. D. McCombe and G. Brozak, to be published.
13. J. P. Cheng and B. D. McCombe, Phys. Rev. Lett. 62, 1925 (1989).
14. D. R. Cohn, D. M. Larsen and B. Lax, Phys. Rev. B 6, 1367 (1972).
15. D. L. Lin, R. Chen and T. F. George, to be published.

TECHNICAL REPORT DISTRIBUTION LIST, GEN

	No. Copies		No. Copies
Office of Naval Research Attn: Code 1113 800 N. Quincy Street Arlington, Virginia 22217-5000	2	Dr. David Young Code 334 NORDA NSTL, Mississippi 39529	1
Dr. Bernard Douda Naval Weapons Support Center Code 50C Crane, Indiana 47522-5050	1	Naval Weapons Center Attn: Dr. Ron Atkins Chemistry Division China Lake, California 93555	1
Naval Civil Engineering Laboratory Attn: Dr. R. W. Drisko, Code L52 Port Hueneme, California 93401	1	Scientific Advisor Commandant of the Marine Corps Code RD-1 Washington, D.C. 20380	1
Defense Technical Information Center Building 5, Cameron Station Alexandria, Virginia 22314	12 high quality	U.S. Army Research Office Attn: CRD-AA-IP P.O. Box 12211 Research Triangle Park, NC 27709	1
DTNSRDC Attn: Dr. H. Singerman Applied Chemistry Division Annapolis, Maryland 21401	1	Mr. John Boyle Materials Branch Naval Ship Engineering Center Philadelphia, Pennsylvania 19112	1
Dr. William Tolles Superintendent Chemistry Division, Code 6100 Naval Research Laboratory Washington, D.C. 20375-5000	1	Naval Ocean Systems Center Attn: Dr. S. Yamamoto Marine Sciences Division San Diego, California 91232	1
		Dr. David L. Nelson Chemistry Division Office of Naval Research 800 North Quincy Street Arlington, Virginia 22217	1

ABSTRACTS DISTRIBUTION LIST, 056/625/629

Dr. J. E. Jensen
Hughes Research Laboratory
3011 Malibu Canyon Road
Malibu, California 90265

Dr. J. H. Weaver
Department of Chemical Engineering
   and Materials Science
University of Minnesota
Minneapolis, Minnesota 55455

Dr. A. Reisman
Microelectronics Center of North Carolina
Research Triangle Park, North Carolina
   27709

Dr. M. Grunze
Laboratory for Surface Science and
      Technology
University of Maine
Orono, Maine 04469

Dr. J. Butler
Naval Research Laboratory
Code 6115
Washington D.C. 20375-5000

Dr. L. Interante
Chemistry Department
Rensselaer Polytechnic Institute
Troy, New York 12181

Dr. Irvin Heard
Chemistry and Physics Department
Lincoln University
Lincoln University, Pennsylvania 19352

Dr. K.J. Klaubunde
Department of Chemistry
Kansas State University
Manhattan, Kansas 66506

Dr. C. B. Harris
Department of Chemistry
University of California
Berkeley, California 94720

Dr. F. Kutzler
Department of Chemistry
Box 5055
Tennessee Technological University
Cookesville, Tennessee 38501

Dr. D. DiLella
Chemistry Department
George Washington University
Washington D.C. 20052

Dr. R. Reeves
Chemistry Department
Renssaeler Polytechnic Institute
Troy, New York 12181

Dr. Steven M. George
Stanford University
Department of Chemistry
Stanford, CA 94305

Dr. Mark Johnson
Yale University
Department of Chemistry
New Haven, CT 06511-8118

Dr. W. Knauer
Hughes Research Laboratory
3011 Malibu Canyon Road
Malibu, California 90265

ABSTRACTS DISTRIBUTION LIST, 056/625/629

Dr. G. A. Somorjai
Department of Chemistry
University of California
Berkeley, California 94720

Dr. J. Murday
Naval Research Laboratory
Code 6170
Washington, D.C. 20375-5000

Dr. J. B. Hudson
Materials Division
Rensselaer Polytechnic Institute
Troy, New York 12181

Dr. Theodore E. Madey
Surface Chemistry Section
Department of Commerce
National Bureau of Standards
Washington, D.C. 20234

Dr. J. E. Demuth
IBM Corporation
Thomas J. Watson Research Center
P.O. Box 218
Yorktown Heights, New York 10598

Dr. M. G. Lagally
Department of Metallurgical
  and Mining Engineering
University of Wisconsin
Madison, Wisconsin 53706

Dr. R. P. Van Duyne
Chemistry Department
Northwestern University
Evanston, Illinois 60637

Dr. J. M. White
Department of Chemistry
University of Texas
Austin, Texas 78712

Dr. D. E. Harrison
Department of Physics
Naval Postgraduate School
Monterey, California 93940

Dr. R. L. Park
Director, Center of Materials
  Research
University of Maryland
College Park, Maryland 20742

Dr. W. T. Peria
Electrical Engineering Department
University of Minnesota
Minneapolis, Minnesota 55455

Dr. Keith H. Johnson
Department of Metallurgy and
  Materials Science
Massachusetts Institute of Technology
Cambridge, Massachusetts 02139

Dr. S. Sibener
Department of Chemistry
James Franck Institute
5640 Ellis Avenue
Chicago, Illinois 60637

Dr. Arnold Green
Quantum Surface Dynamics Branch
Code 3817
Naval Weapons Center
China Lake, California 93555

Dr. A. Wold
Department of Chemistry
Brown University
Providence, Rhode Island 02912

Dr. S. L. Bernasek
Department of Chemistry
Princeton University
Princeton, New Jersey 08544

Dr. W. Kohn
Department of Physics
University of California, San Diego
La Jolla, California 92037

ABSTRACTS DISTRIBUTION LIST, 056/625/629

Dr. F. Carter
Code 6170
Naval Research Laboratory
Washington, D.C. 20375-5000

Dr. Richard Colton
Code 6170
Naval Research Laboratory
Washington, D.C. 20375-5000

Dr. Dan Pierce
National Bureau of Standards
Optical Physics Division
Washington, D.C. 20234

Dr. R. Stanley Williams
Department of Chemistry
University of California
Los Angeles, California 90024

Dr. R. P. Messmer
Materials Characterization Lab.
General Electric Company
Schenectady, New York 22217

Dr. Robert Gomer
Department of Chemistry
James Franck Institute
5640 Ellis Avenue
Chicago, Illinois 60637

Dr. Ronald Lee
R301
Naval Surface Weapons Center
White Oak
Silver Spring, Maryland 20910

Dr. Paul Schoen
Code 6190
Naval Research Laboratory
Washington, D.C. 20375-5000

Dr. John T. Yates
Department of Chemistry
University of Pittsburgh
Pittsburgh, Pennsylvania 15260

Dr. Ric   Greene
Code 52
Naval Resear   Laboratory
Washington, D.C. 20375-5000

Dr. L. Kesmodel
Department of Physics
Indiana University
Bloomington, Indiana 47403

Dr. K. C. Janda
University of Pittsburg
Chemistry Building
Pittsburg, PA 15260

Dr. E. A. Irene
Department of Chemistry
University of North Carolina
Chapel Hill, North Carolina 27514

Dr. Adam Heller
Bell Laboratories
Murray Hill, New Jersey 07974

Dr. Martin Fleischmann
Department of Chemistry
University of Southampton
Southampton 509 5NH
UNITED KINGDOM

Dr. H. Tachikawa
Chemistry Department
Jackson State University
Jackson, Mississippi 39217

Dr. John W. Wilkins
Cornell University
Laboratory of Atomic and
  Solid State Physics
Ithaca, New York 14853

ABSTRACTS DISTRIBUTION LIST, 056/625/629

Dr. R. G. Wallis
Department of Physics
University of California
Irvine, California 92664

Dr. D. Ramaker
Chemistry Department
George Washington University
Washington, D.C. 20052

Dr. J. C. Hemminger
Chemistry Department
University of California
Irvine, California 92717

Dr. T. F. George
Chemistry Department
University of Rochester
Rochester, New York 14627

Dr. G. Rubloff
IBM
Thomas J. Watson Research Center
P.O. Box 218
Yorktown Heights, New York 10598

Dr. Horia Metiu
Chemistry Department
University of California
Santa Barbara, California 93106

Dr. W. Goddard
Department of Chemistry and Chemical
   Engineering
California Institute of Technology
Pasadena, California 91125

Dr. P. Hansma
Department of Physics
University of California
Santa Barbara, California 93106

Dr. J. Baldeschwieler
Department of Chemistry and
   Chemical Engineering
California Institute of Technology
Pasadena, California 91125

Dr. J. T. Keiser
Department of Chemistry
University of Richmond
Richmond, Virginia 23173

Dr. R. W. Plummer
Department of Physics
University of Pennsylvania
Philadelphia, Pennsylvania 19104

Dr. E. Yeager
Department of Chemistry
Case Western Reserve University
Cleveland, Ohio 41106

Dr. N. Winograd
Department of Chemistry
Pennsylvania State University
University Park, Pennsylvania 16802

Dr. Roald Hoffmann
Department of Chemistry
Cornell University
Ithaca, New York 14853

Dr. A. Steckl
Department of Electrical and
   Systems Engineering
Rensselaer Polytechnic Institute
Troy, NewYork 12181

Dr. G.H. Morrison
Department of Chemistry
Cornell University
Ithaca, New York 14853